

Example-Based Framework for Perceptually Guided Audio Texture Generation

Purnima Kamath*, Chitralekha Gupta* *Member IEEE*, Lonce Wyse† *Member IEEE*, Suranga Nanayakkara*

†Universitat Pompeu Fabra

*National University of Singapore

Corresponding Author: purnima.kamath@u.nus.edu

Abstract—Generative models for synthesizing audio textures explicitly encode controllability by conditioning the model with labelled data. While datasets for audio textures can be easily recorded in-the-wild, semantically labeling them is expensive, time-consuming, and prone to errors due to human annotator subjectivity. Thus, to control generation, there is a need to automatically infer user-defined perceptual factors of variation in the latent space of a generative model while modelling unlabeled textures. In this paper, we propose an example-based framework to determine vectors to guide texture generation based on user-defined semantic attributes. By synthesizing a few synthetic examples to indicate the presence or absence of a semantic attribute, we can infer the guidance vectors in the latent space of a generative model to control that attribute during generation. Our results show that our method is capable of finding perceptually relevant and deterministic guidance vectors for controllable generation for both discrete as well as continuous textures. Furthermore, we demonstrate the application of this method to other tasks such as selective semantic attribute transfer.

Index Terms—Audio Textures, Controllability, Analysis-by-Synthesis, Gaver Sounds, StyleGAN, Latent Space Exploration

I. INTRODUCTION

Audio textures are sounds generated by the super-position of multiple similar acoustic events [1], [2], such as the sounds made by water filling a container or a wooden drumstick repeatedly hitting a metallic surface. Guided or controllable generation of such audio textures using deep neural networks is useful for generating background environmental sound scores for movies, games, and automated Foley sound synthesis [3], [4], [5]. Such guidance during generation is usually achieved by conditioning generative models using semantically labeled data. While large datasets for audio textures can be readily recorded in-the-wild, semantically labeling these kinds of sounds is difficult. There is thus a need for generative models to infer the vectors for semantic attribute guidance automatically, without the supervision of large labeled datasets.

Generative adversarial networks (GANs) [6] such as StyleGANs [7], [8] generate disentangled latent spaces by learning the most statistically significant factors of variation within a dataset. Algorithms in the image domain [9], [10], statistically analyse such latent spaces to automatically find guidance vectors for controllable generation. Ideally, controllable generation should operate at a perceptual or a human-understandable semantic level [11]. We define semantic attributes in audio as a set of factors that matter to human perception of sound. Such

attributes may not always have a one-to-one correspondence to the statistically found guidance vectors. Thus, sound design processes would be greatly improved by intuitive user-defined semantic guidance vectors for controllable audio textures generation.

Recent research has focused on describing semantic attributes to guide audio generation using text or language abstractions [12], [13], [14], [15]. This multi-modal guidance is achieved by training generative models on large audio datasets in conjunction with text annotations such as captions [16], [17]. While abstracting control using such language-based prompts is a step towards generalized sound generation, it is difficult to use text for fine-grained and continuous controls required for applications of audio texture synthesis.

In this paper, we propose using audio examples to guide latent space access and navigation. Similar to music information retrieval (MIR) techniques such as query-by-example [18], [19], [20], [21] and query-by-humming [22], [23], [24], [25] we generate synthetic sound examples representative of the semantic attribute we want to control during generation. We encode these examples into the latent space of a GAN unconditionally trained on real-world audio textures. Then we use these latent embeddings to define guidance vectors in the latent space along which desired semantic attributes can be systematically varied during texture generation. As shown on our webpage¹, we use these guidance vectors to guide texture generation for various user-defined semantic attributes such as “Brightness”, “Rate” or “Impact Type” for discrete impact sounds and “Fill-Level” for the continuous texture of water filling.

We validate the effectiveness of our method for user-defined semantic guidance of texture generation through a comprehensive attribute rescoring analysis. We also conduct perceptual listening tests to evaluate the effectiveness of our method in changing specific attributes for various randomly generated sounds. In summary, our contributions are:

- An Example-Based Framework (EBF) to find user-defined attribute guidance vectors to semantically control audio texture generation.
- A synthetic audio query approach for latent space exploration of a generative model.
- An application of our framework for the task of semantic attribute transfer between textures.

¹<https://augmented-human-lab.github.io/audio-guided-generation/>

II. RELATED WORK

A. Supervised Controllability in Audio

Generative models for audio [26], [27], [28], [29], [30], [31], [32], [33], [34], [35], [36] enable controllability by training on datasets with labels that help organize the latent space according to the timbre-specific features in the datasets. Some datasets, especially in the area of music generation, are labelled during dataset creation [28], others are weakly labelled by crowdsourcing [37] or are inferred from the audio samples themselves. GANSynth [26] uses instrument identifiers and musical pitch conditioning to generate and interpolate between various musical instrument timbres. DDSP [27] integrates classic signal processing algorithms with deep neural networks to build differentiable synthesizers with latent representations for attributes such as pitch or loudness to guide generation. In DrumGAN [38], a Progressive GAN (PGAN) [39] is trained on drum sounds labeled with features extracted automatically using Audio Commons [40] and Essentia [41]. Features such as hardness, sharpness or warmth of the sound can then be used to control generation. In DarkGAN [42], a Progressive GAN is trained on soft labels distilled from an audio tagging classifier [43] trained on tags from the AudioSet ontology. Esling et. al [44], [45] construct generative timbre spaces regularized using similarity ratings collected via perceptual studies that can be used for controllable, descriptor-based sound synthesis.

In the domain of audio texture generation, MorphGAN [46] trains on floating-point class and parameter labels generated from the penultimate layer of a classifier which can then generate smooth inter-class and intra-class morphs. The Sound Model Factory [47] trains a GAN which is used to create novel timbres followed by an RNN trained on sounds produced from the GAN and conditioned on points along smoothly parameterized trajectories through the GAN latent space. All of these supervised training methods rely on additional class or parametric information while training generative algorithms. Since GANs, particularly StyleGANs, are able to disentangle the latent space based on semantics in the training data [7], our research explores finding user-defined semantic directions to guide generation without the need for any explicit conditioning or labelled data during training.

B. Unsupervised Controllability

In computer vision, algorithms such as [9], [10], [48], [49], [50], [51] leverage StyleGANs ability to disentangle the latent space to find directional vectors for editing semantics on images. Similarly in audio, GANSpaceSynth [52] applies the GANSpace algorithm to control a pre-trained GANSynth trained on musical instruments in an unsupervised manner. More recently, in computer vision, Semantic Factorization (SeFa) [10] was shown to perform better than other unsupervised algorithms to find vectors for controllable generation in the latent space of a pre-trained GAN. In this method, the weights of the layers that create the disentangled representation are decomposed to find the vectors for maximum variation. Such vectors are then used to edit semantics on unconditionally generated images. However, the directional

vectors generated using SeFa need to be semantically labelled manually after observing edits across multiple samples.

For speech and music [53], [54] infer controllability based on supervision from a few labels. For images, FLAME [55] uses supervision from a few positive-negative image pairs by semantically editing and inverting real images in a StyleGAN's latent space. Direction vectors for semantic attribute editing are found by optimizing for cosine similarity between the pairs' difference vectors. In our work, we modify the FLAME method for audio textures and propose using a few fully synthetically generated examples to assist in deriving vectors in the latent space of a GAN for attribute controllability. A cluster of similar synthesized audio examples is inverted [56], [57] to define clusters in the GAN's latent space. A prototype [58] latent vector is derived from each cluster, and is an abstract average of the semantic cluster they represent. Since such prototypes are designed to differ in a specific attribute, the difference vector between them in the latent space can be used for guiding audio texture synthesis and for semantic attribute transfer.

C. Synthetic Texture Generation

While real-world sounds could also be inverted to find latent representations in a trained GAN, they are much more difficult to control than parametric acoustic sound synthesizers [59], [60], [61], [62] or physics-based models [63]. For our inharmonic textures, we use a physically informed synthesis technique found in William Gaver's seminal work on auditory perception [64], [65]. His approach is based on the idea that humans hear and describe sound events in terms of their sources and source attributes better than in terms of acoustic properties of the sounds themselves. The sound events in Gaver sounds are modeled on the physics of the objects interacting to produce the sound such as the hardness of the material under impact or the force of impact. Gaver [64] refers to analysis-by-synthesis as a process of updating synthesis parameters to match a target sound, which we use to discover GAN latent vectors with synthetic audio queries.

Although algorithmically synthesized sounds can sound unnatural, we employ them only for querying and searching the latent space of a GAN. Multi-event synthetic textures can be quickly and easily generated using an analysis-by-synthesis approach that have attributes adequate for this exploration task.

III. PROPOSED FRAMEWORK

As shown in Figure 1 a, b and c, we partition our goal to find semantic attribute vectors for controllable texture generation and propose a framework comprised of the following modules:

- A Generator module (G) of a GAN trained on real-world audio for high fidelity texture synthesis,
- A GAN Encoder (E), also known as a GAN inversion network, to encode an audio example into the latent space of a pre-trained GAN,
- A parametric Gaver synthesizer for sounds used to locate desired points in the latent space of the GAN,
- An algorithm to derive semantic attribute clusters and prototype vectors for guiding semantic synthesis trajectories in the latent space of the GAN.

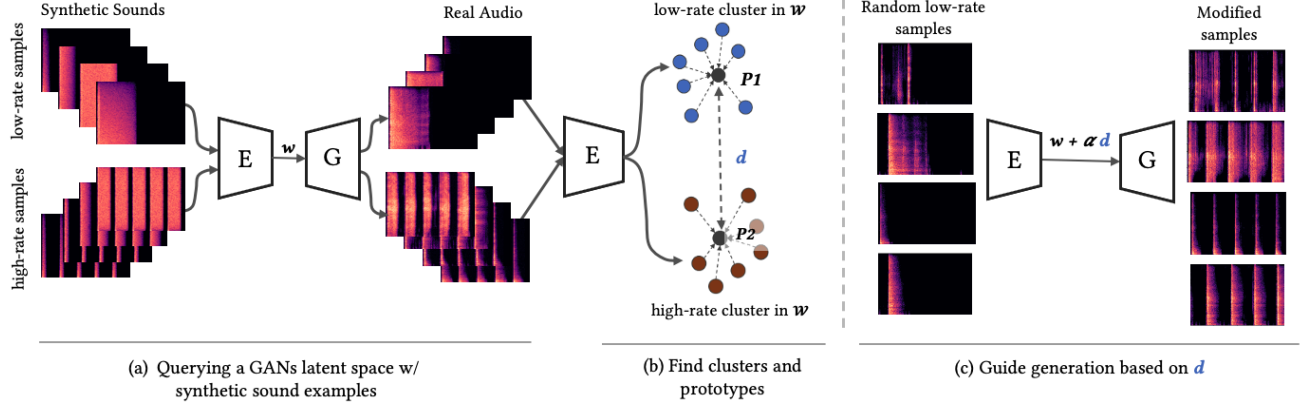


Fig. 1: A schematic diagram outlining our framework during inference.

Figure 1 illustrates our framework (during inference). G is a GAN generator and E is the GAN Encoder. (a) We generate synthetic Gaver sounds for a semantic attribute we want to control. In the diagram above we demonstrate this using “Rate” or number of impact sounds in a sample as the semantic attribute. We encode these synthetic sound examples into the latent space of a GAN to find their w -embeddings. (b) Next, we derive the semantic attribute clusters and generate prototypes using the algorithms elaborated in section III-D. The direction vector to guide generation for that semantic concept is indicated by “ d ”. (c) Shows how we can use direction vector “ d ” to guide generation on any randomly generated audio sample to increase or decrease “Rate”.

A. GAN for Audio Textures

While our framework can be applied to derive attribute guidance vectors for both Progressive GANs or StyleGANs for audio, in this paper we demonstrate this using StyleGAN2 [7] trained on audio textures. A StyleGAN2’s generator can be modeled as a function $G(\cdot)$ that maps a δ_z -dimensional latent space $z \subseteq Z, z \in \mathbb{R}^{\delta_z}$ to the higher dimensional spectrogram space $s \subseteq S, s \in \mathbb{R}^{f \times t}$, such that $s = G(z)$. Here δ_z is the dimensionality of the Z space and f, t are the number of frequency channels and time frames of the generated spectrogram respectively. StyleGANs further learn an intermediate representation $w \subseteq \mathcal{W}, w \in \mathbb{R}^{\delta_w}$ between that of Z and S via a mapping network $G_m(\cdot)$ which further disentangles factors of variation as compared to the latent Z space. Further, a synthesis network $G_s(\cdot)$ maps the w vector to the spectrogram S space. Our framework and method operates in the \mathcal{W} space to find semantically meaningful directions for controllability.

B. GAN Encoder

While GANs learn to map latent space embeddings to real-world sounds, GAN inversion techniques learn the inverse mapping, i.e., from the real-world sounds to the latent space embeddings. We adapt the encoder model from [57] to estimate a w vector from an audio spectrogram randomly sampled from a pre-trained StyleGAN2. Previously, [66], [67] have shown that masking techniques are effective while learning generalized vector representations for audio. We extend this idea of arbitrarily masking the spectrogram to learn a w vector representation. This approach is especially useful during

inference to generalize the encoder to synthetic Gaver sounds. It assists in projecting the synthetic sounds into a reasonable part of the latent space even though the encoder (or the GAN) is not directly trained on these sounds.

For noisy textures, such as the sounds made by water filling a container, we further employ amplitude thresholding of the spectrogram during training. This thresholding ensures that the encoder ignores the low level noise and focuses on the most prominent events and frequencies in the spectrogram while estimating the w vector. To train the Encoder, we modify the loss function from [57] to estimate only in the \mathcal{W} space instead of Z as:

$$\mathcal{L} = \mathbb{E}_{z \sim \mathcal{N}(0,1), w=G_m(z), s=G_s(w)} [\|s - G_s(E(s))\|_2^2 + \|w - E(s)\|_2^2] \quad (1)$$

In Equation 1, $G_m(z)$ is the mapping network, $G_s(w)$ is the synthesis network of the StyleGAN2, $E(s)$ is the Encoder that inverts the spectrogram s to the \mathcal{W} space. While training the encoder, we randomly sample a z from the Z space to generate the target spectrogram s using $G(z)$. We estimate the w for this spectrogram using the encoder $E(s)$. For the first loss term, we pass the inverted w through the synthesis network of the generator $G_s(w)$ and find the mean squared error (MSE) loss between the original and reconstructed samples. The second term is the MSE loss between the actual and the estimated w vector.

The loss function of the original Encoder algorithm [57] additionally used a perceptual similarity loss term called LPIPS [68] that calculates the distance between image patches in order to preserve the perceptual similarity of the estimated images. Unlike images, the spectrograms of audio textures are characterized by temporal similarity due to the parameters that remain constant over time [1]. In our experiments, in addition to Equation 1, to preserve the temporal structure of the generated sounds, we use a Gram Matrix feature based autocorrelation loss term suggested by Antognini et al. [69] instead of LPIPS -

$$\mathcal{L}_{\text{autocorr}} = \frac{\sum_{k,\mu} (\mathcal{A}_\mu^k - \tilde{\mathcal{A}}_\mu^k)^2}{\sum_{k,\mu} (\tilde{\mathcal{A}}_\mu^k)^2} \quad \text{where } \mathcal{A}_\mu^k = \mathcal{F}_f^{-1} [\mathcal{F}_t[F_\mu^k] \mathcal{F}_t[F_\mu^k]^*] \quad (2)$$

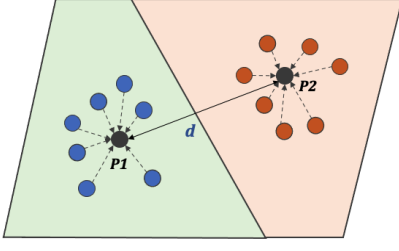


Fig. 2: Schematic for generating semantic attribute clusters, prototypes and the direction vector.

In Equation 2, F_μ^k is the k th feature map for filter μ , A_τ^k is the autocorrelation of the k th feature map, \mathcal{F} represents the Fourier transform and $*$ represents its complex conjugation. As shown in [69], such an autocorrelation loss assists in preserving the periodic structure in the resulting sounds.

C. Synthesizing Gaver Sounds

To generate audio examples for querying the GAN latent space, we use two Gaver synthesis methods - (1) based on physical parameters of the interacting objects, and (2) based on object resonance as a series of band pass filters. The first method is useful in generating sharp impact sounds or dripping sounds, and the second for producing larger variety of impacts and scraping sounds. More formally, a synthetic impact sound can be described as $F(t) = \sum_n \phi_n e^{\delta_n t} \cos \omega_n t$, where $F(t)$ describes the generated sound, ϕ_n is the amplitude of the n th partial, δ_n is a damping constant, and ω is the frequency of the partial, \sum signifies a sum over the total number of partials. From an ecological perspective, each component in the equation controls a physical aspect of the objects interacting to generate the impact sound. For instance, δ in the equation controls the material hardness, ϕ controls the force of impact, and ω and n control the size of the object. With method 2, impact and scraping sounds are created by passing Gaussian noise $\mathcal{N}(0, I)$ through band-pass and fade filters. The amplitude of the impact sound governs the force of impact, while the frequency bands together with damping provided by linear or exponential fade filters govern the material of impact of the sound.

D. Semantic Clusters, Prototypes, and Guidance Vectors

Having generated synthetic Gaver sounds, we invert them to generate the w embeddings. We then cluster the sounds together in the \mathcal{W} space to generate prototypes as shown in Figure 2.

Assume for example that we want to derive directional vectors to control the attribute of “Brightness” of an impact sound. We define brightness as an attribute to indicate the presence or absence of high frequency components in a sound. We generate a cluster of Gaver sounds where the semantic attribute is present (represented by blue dots in the figure) and another cluster of Gaver sounds where the semantic attribute is absent (or “dull” impact sounds represented by orange dots). We find the prototypes **P1** and **P2** representative of each semantic attribute cluster using Algorithm 1. The direction vector for editing the semantic attribute is given by the difference vector between **P1** and **P2**.

Algorithm 1: Get Prototype

Input:

$\{w_0, \dots, w_n\}$ or $List(w_n)$ is list of encoded synthetic samples for a semantic attribute, where $w_n \in \mathbb{R}^{\delta_w}$;
 w_avg is the centre of mass of \mathcal{W} space;

Output:

w_ptype the prototype representation

Function $GetPrototype(List(w_n), w_avg)$:

```

 $w \leftarrow List(w_n) - w\_avg$ ;
 $U, S, V \leftarrow SVD(w)$ ;
 $w\_ptype \leftarrow w\_avg + U_s \cdot U_s^T \cdot \bar{w}$ ;
    ;  $\bar{w}$  is mean  $List(w_n)$ 
    ;  $U_s \leftarrow U[\argmax(S)]$ 

```

return w_ptype

To generate our prototypes, we adapt a technique from computer vision for generating Eigenfaces. We stack all w embeddings for the synthetic Gaver samples in a semantic cluster together as columns of a matrix and perform singular value decomposition and select the component associated with the maximum singular value to construct the prototype. The intuition behind doing this is that after decomposition the component with the highest singular value has the most common prominent feature amongst all the samples being analyzed, i.e. the semantic attribute being modelled. Constructing an “average” prototype this way is more robust to outliers or artificial synthesis artefacts. The direction vector for edits is the difference between the w embeddings of the two prototypes as shown in Algorithm 2. This direction vector can be used to continuously and sequentially edit the semantic attribute of any randomly generated sample.

Algorithm 2: Get Attribute Guidance Vector

Input:

$List(s_{1_n})$ is list of synthetic spectrogram indicating attribute presence (for P1 prototype), $s_{1_n} \in \mathbb{R}^{f \times t}$;
 $List(s_{2_n})$ is list of synthetic spectrogram indicating attribute absence (for P2 prototype), $s_{2_n} \in \mathbb{R}^{f \times t}$;
 w_avg is the centre of mass of \mathcal{W} space;

Output:

$direction$ attribute guidance vector

Function $GetDirection(List(s_{1_n}), List(s_{2_n}), w_avg)$:

```

 $\{w_{1_0}, \dots, w_{1_n}\} \leftarrow E(s_{1_0}, \dots, s_{1_n})$  ;  $\blacktriangleright$  encode into  $\mathcal{W}$ 
 $\{w_{2_0}, \dots, w_{2_n}\} \leftarrow E(s_{2_0}, \dots, s_{2_n})$ ;

```

```

 $w_{1\_prototype} \leftarrow GetPrototype(\{w_{1_0}, \dots, w_{1_n}\})$ ;
 $w_{2\_prototype} \leftarrow GetPrototype(\{w_{2_0}, \dots, w_{2_n}\})$ ;

```

```

 $direction \leftarrow w_{1\_prototype} - w_{2\_prototype}$ ;

```

return $direction$

IV. EXPERIMENTS

A. Datasets

We use two audio texture datasets in our experiments: (1) The Greatest Hits dataset [70] to demonstrate the effectiveness

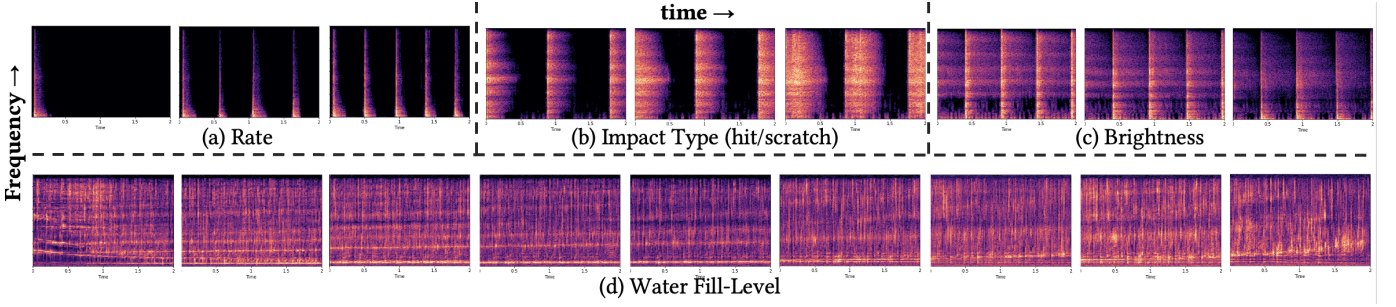


Fig. 3: (Top Row) Spectrogram examples of guided generation using our method based on change in the attributes of (a) Rate (increases L to R), (b) Impact Type (becomes scratchy L to R), and (c) Brightness (decreases L to R). Note that for each example, as one attribute changes the other attributes do not undergo a change. (Bottom Row) Examples of guided generation for water filling a container based on Fill-Level. Note how the Fill-Level and its respective frequency components gradually increase from L to R. All sounds can be auditioned on our webpage <https://augmented-human-lab.github.io/audio-guided-generation/>.

of our approach on discrete impact sounds and (2) a Water filling a container dataset [71] for continuous and noisy audio textures. Through these two datasets we demonstrate the effectiveness of our method to cover a range of discrete and continuous textures.

1) *The Greatest Hits Dataset*: This dataset contains audio and video recordings of a wooden drumstick probing indoor and outdoor environments by hitting, scraping, and poking different objects of different material densities. We use this dataset to explore the rich timbres arising out of the interactions between the wooden drumstick and various hard and soft surfaces such as tree trunks, dirt, leaves, metal cans, ceramic mugs, carpets, soft cushions etc. The dataset contains approximately 10 hours of denoised audio split into 977 audio files each approximately 35 seconds. Each file contains impact sounds interacting with different types of objects. We split the audio files into consecutive 2 second sounds sampled at 16kHz to unconditionally train our StyleGAN2. We develop semantic attribute clusters, prototypes and attribute guidance vectors for the attributes **Brightness** (whether the sound contains mostly high frequency components or is dark or dull containing mostly low frequency components), **Rate** (whether the number of impact sounds in a sample is high or low), and **Impact Type** (whether the sounds are sharp impacts or scraping/scratchy sounds made by dragging the stick across the surface).

2) *Water filling a container*: This dataset [71] contains 50 audio recordings of water filling a container at an approximately constant rate for an average duration of ~ 30 seconds. We develop semantic attribute clusters, prototypes and attribute guidance vectors for the continuously varying attribute of **Fill-Level** of the container. We sample the recorded audio files using a sliding window of 100ms to generate approximately 10,000 2-second audio files sampled at 16kHz to unconditionally train our StyleGAN2. We choose a small sliding window size of 100ms to achieve better interpolatability [11] for **Fill-Level** in the \mathcal{W} space of the GAN.

B. Implementation Details

StyleGAN2: We set Z and \mathcal{W} space dimensions δ_z and δ_w both to 128 and use 4 mapping layers in the Generator for all our experiments. Further, we use the log-magnitude spectrogram representations generated using a Gabor transform [29] ($n_frames = 256$, $stft_channels = 512$, $hop_size =$

128), a Short-Time Fourier Transform (STFT) with a Gaussian window, to train the StyleGAN2 and the Phase Gradient Heap Integration (PGHI) [72] for high-fidelity spectrogram inversion of textures to audio [73]. For training the generator and discriminator of the StyleGAN2 we use an Adam optimizer with a learning rate of 0.0025, β_1 as 0.0 and β_2 as 0.99.

Encoder Training: We use a ResNet-34 [74] backbone as the architecture for our GAN Encoder network. We use an amplitude thresholding of -17db for Water and -25db for the Greatest Hits. That is, we mask the frequency components with magnitude below -17 or -25db for the respective datasets. We use an Adam optimizer to train the Encoder with a learning rate of 0.00001, β_1 as 0.5, and β_2 as 0.99.

Gaver Sound Synthesis: In all our experiments, we use 10 synthetic Gaver examples (5 per semantic attribute cluster) to generate the guidance vectors for controllable generation. We outline a cluster-based analysis for real and synthetic sounds using UMAP visualizations on our supplementary webpage.

C. Evaluation metric

For audio quality we utilize the *Fréchet Audio Distance* [75] (FAD) metric. FAD is the distance between the distribution of the embeddings of real and synthesized audio data extracted from a pre-trained VGGish model. We utilize this metric to evaluate the quality of sounds generated by inverting the synthetic Gaver sounds as well as real-world sounds from the latent space of the GAN.

To evaluate the effectiveness of our method in changing a semantic attribute of a texture we perform *rescoring analysis*. By *rescoring*, we mean the change in accuracy scores reported by an attribute classifier before and after the change in the semantic attribute on a sound. For this, we train an attribute presence or absence classifier based on [76]. We then manipulate an attribute on some sounds and observe how the classifier score changes for those sounds. Further, we evaluate if the attribute change occurs without modifying other attributes. For instance, when editing **Brightness**, we first analyse if the intended attribute of brightness changes. We then analyse if other attributes such as **Rate** changes with it.

As our datasets are unlabelled, to train the *rescoring analysis* classifier, we manually curate and label a small subset of sounds. To do this, we selected approximately 250 samples

TABLE I: Ablation Studies

| | Greatest Hits | | | | | | Water |
|----------------------------------|-----------------------------------|-----------------------------------|-----------------------------------|-----------------------------------|-----------------------------------|-----------------------------------|-----------------------------------|
| | Brightness | | Rate | | Impact Type | | Fill-Level |
| | Acc.(\uparrow) | Avg. Chng Others (\downarrow) | Acc.(\uparrow) | Avg. Chng Others (\downarrow) | Acc.(\uparrow) | Avg. Chng Others (\downarrow) | Acc.(\uparrow) |
| EBF: MSE+LPIPS [68] | 0.53 ± 0.08 | 0.24 ± 0.04 | 0.64 ± 0.08 | 0.35 ± 0.07 | 0.69 ± 0.07 | 0.20 ± 0.04 | 0.60 ± 0.1 |
| EBF: MSE+GM AutoCorrelation [69] | 0.79 ± 0.06 | 0.21 ± 0.06 | 0.85 ± 0.06 | 0.45 ± 0.09 | 0.46 ± 0.07 | 0.49 ± 0.07 | 0.77 ± 0.09 |
| EBF: MSE (Ours) | 0.71 ± 0.06 | 0.14 ± 0.03 | 0.88 ± 0.06 | 0.30 ± 0.07 | 0.81 ± 0.04 | 0.24 ± 0.4 | 0.27 ± 0.1 |
| EBF: MSE (Ours) + Thresholding | 0.82 ± 0.05 | 0.21 ± 0.06 | 0.89 ± 0.06 | 0.35 ± 0.1 | 0.80 ± 0.06 | 0.27 ± 0.06 | 0.97 ± 0.04 |

TABLE II: FAD Scores for GAN generated sounds and Encoder reconstructions

| | Greatest Hits | | | Water | | |
|----------------------------------|---------------|----------------------------|------------------------------|-------|----------------------------|------------------------------|
| | GAN | GAN Recon.(\downarrow) | Gaver Recon.(\downarrow) | GAN | GAN Recon.(\downarrow) | Gaver Recon.(\downarrow) |
| EBF: MSE+LPIPS [68] | 0.6 | 1.12 | 4.40 | 1.17 | 1.92 | 9.45 |
| EBF: MSE+GM AutoCorrelation [69] | | 1.27 | 4.27 | | 9.22 | 8.26 |
| EBF: MSE (Ours) | | 0.72 | 4.61 | | 1.59 | 11.77 |
| EBF: MSE (Ours) + Thresholding | | 2.83 | 4.16 | | 1.42 | 7.92 |

of 2 seconds sounds for each semantic attribute under consideration. This manual curation involved visually analysing the video and auditioning the associated sounds to detect the semantic attribute. For more details on the dataset curation please see our webpage. Note that this curated dataset is only used for quantitative analysis and not used to train our GAN or Encoder models.

D. Baseline Selection

We evaluate our method’s effectiveness in finding user-defined attribute guidance vectors in the latent space of the GAN by comparing it with an unsupervised method for latent semantic discovery called closed-form Semantic Factorization (SeFa) [10]. SeFa decomposes the pre-trained weights of a GAN to find statistically significant vectors for guided generation. Although SeFa is relatively under-studied in the domain of audio, we use it as a baseline for comparison because, like our method, SeFa works on unconditionally trained GANs. Given the novelty of our task in deriving guidance vectors in a post-hoc fashion, to the best of our knowledge, the SeFa method is the state-of-the-art method in this regard. We thus use it for comparison.

E. Experimental Details

We first conduct ablation studies to understand the effects of individual components of the loss functions outlined in section III-B. We report this analysis using both *rescoring analysis* and *FAD* scores. Next, we study the impact of change of an attribute on other attributes under consideration. We then compare our method (EBF) with the SeFa method as baseline. Finally, we qualitatively study the effectiveness of our method by conducting listening tests. We also present an interactive interface to demonstrate the practicality and effectiveness of our method. Figure 3 shows some spectrogram examples of guided generation using our method. The standard error of means in all tables in this section were reported by bootstrapping the samples over 100 iterations.

1) *Ablation Studies*: We conduct two types of ablation studies in our paper - (1) to study the effect of different components of the loss function on the Encoder, and (2) to

study the effect of number of synthetic samples needed to create a semantic cluster.

Ablating Encoder Loss Components: We first study the effect of using LPIPS, autocorrelation, and MSE loss terms while training the Encoder. Table I shows the *rescoring* accuracy scores for attribute changes for each type of Encoder. (\uparrow) indicates higher values are better. For each attribute change we report the accuracy for the main attribute as well as the average change reported in other attributes. Ideally, we would like the main attribute accuracy to be high and change in other attributes to be low. We find that with MSE+GM autocorrelation loss, the system outperforms the one with MSE+LPIPS loss for the attributes brightness, rate, and fill-level possibly because with autocorrelation loss, the Encoder is able to preserve the frequency components and the occurrence of sharp attack transients in the resulting sounds, but is unable to preserve the impulse width of the impact in the time domain. Further, given the scope of our Encoder to invert synthetic sounds to derive guidance vectors, we find that for Greatest Hits dataset, using an Encoder with MSE-only, with or without thresholding, works best and is sufficient as compared to others. Also, the average change in other attributes for both the MSE-only based Encoders are comparable (means are within one standard error of each other). For Water, using an Encoder with MSE and thresholding works best.

Table II shows the FAD scores for GAN generated sounds (column called GAN) and Encoder reconstructions for each type of Encoder for both GAN generated sounds as well as synthetic Gaver sounds. The FAD Scores were computed based on 10,000 randomly generated samples in comparison with the entire training set. We find that the encoder trained using MSE only or MSE+thresholding outperforms the other systems in terms of the quality of the generated audio (FAD scores). Thus, based on this table and Table I, we choose the Encoder with MSE and thresholding as the best performing Encoder for both datasets for the remainder of the paper.

Ablating the Number of Gaver Samples: Next, we study the effect of the number Gaver samples used to find the guidance vectors for different attributes. We derive guidance using different N , starting with $N=1$ to $N=5$. We observe that, as N increases, the effectiveness of the directional vector

TABLE III: Comparison with Baseline

| | Greatest Hits | | | | | | Water |
|--------------------------------|------------------------|-----------------------------------|------------------------|-----------------------------------|------------------------|-----------------------------------|------------------------|
| | Brightness | | Rate | | Impact Type | | Fill-Level |
| | Acc.(\uparrow) | Avg. Chng Others (\downarrow) | Acc.(\uparrow) | Avg. Chng Others (\downarrow) | Acc.(\uparrow) | Avg. Chng Others (\downarrow) | Acc.(\uparrow) |
| SeFa [10] | 0.49 \pm 0.11 | 0.19 \pm 0.12 | 0.45 \pm 0.12 | 0.29 \pm 0.14 | 0.42 \pm 0.15 | 0.31 \pm 0.09 | 0.92 \pm 0.09 |
| EBF: MSE (Ours) + Thresholding | 0.82 \pm 0.05 | 0.21 \pm 0.06 | 0.89 \pm 0.06 | 0.35 \pm 0.10 | 0.80 \pm 0.06 | 0.27 \pm 0.06 | 0.97 \pm 0.04 |

TABLE IV: Pairwise rescoring for Greatest Hits (EBF)

| | Brightness(\uparrow) | Rate(\uparrow) | Impact Type(\uparrow) |
|-------------|--------------------------|------------------------|---------------------------|
| Brightness | 0.82 \pm 0.06 | 0.06 \pm 0.04 | 0.40 \pm 0.07 |
| Rate | 0.40 \pm 0.09 | 0.89 \pm 0.06 | 0.38 \pm 0.09 |
| Impact Type | 0.35 \pm 0.07 | 0.19 \pm 0.03 | 0.80 \pm 0.05 |

TABLE V: Pairwise rescoring for Greatest Hits (SeFa)

| | Brightness(\uparrow) | Rate(\uparrow) | Impact Type(\uparrow) |
|-------------|--------------------------|------------------------|---------------------------|
| Dimension 0 | 0.10 \pm 0.07 | 0.07 \pm 0.06 | 0.18 \pm 0.13 |
| Dimension 1 | 0.30 \pm 0.11 | 0.45 \pm 0.12 | 0.28 \pm 0.16 |
| Dimension 2 | 0.31 \pm 0.11 | 0.09 \pm 0.06 | 0.42 \pm 0.15* |
| Dimension 3 | 0.49 \pm 0.12 | 0.09 \pm 0.06 | 0.30 \pm 0.16 |
| Dimension 4 | 0.12 \pm 0.08 | 0.14 \pm 0.08 | 0.17 \pm 0.12 |
| Dimension 5 | 0.31 \pm 0.11 | 0.10 \pm 0.06 | 0.30 \pm 0.14 |
| Dimension 6 | 0.32 \pm 0.11 | 0.14 \pm 0.08 | 0.19 \pm 0.13 |
| Dimension 7 | 0.14 \pm 0.08 | 0.10 \pm 0.06 | 0.38 \pm 0.16* |
| Dimension 8 | 0.18 \pm 0.09 | 0.09 \pm 0.07 | 0.28 \pm 0.16 |
| Dimension 9 | 0.34 \pm 0.10 | 0.11 \pm 0.07 | 0.20 \pm 0.13 |

TABLE VI: Pairwise rescoring for Water (EBF and SeFa)

| | | SeFa | Fill-Level(\uparrow) |
|------------|--------------------------|-------|--------------------------|
| EBF (ours) | Fill-Level(\uparrow) | Dim 0 | 0.14 \pm 0.11 |
| | | Dim 1 | 0.92 \pm 0.09 |
| | | Dim 2 | 0.27 \pm 0.16 |
| | Fill-Level | | |
| | | | 0.97 \pm 0.04 |

edits also increases. Also, such edits preserve other un-edited attributes better with higher N. The samples with different N's can be auditioned on our supplementary webpage.

2) *Baseline Comparison*: Table III reports the *rescoring analysis* for each attribute using our method in comparison with SeFa. We report both, the score for change in the main intended attribute being edited as well as the average change in other attributes. (\uparrow) indicates higher values are better. For both datasets our method reports better accuracies for change in the main attribute as compared to SeFa.

We further report pairwise attribute edit comparisons to study the effect of change in one attribute individually on every other attribute. Tables IV and V show this for Greatest Hits dataset and Table VI for Water dataset. For SeFa, since we do not know which vector (of the $\delta_w=128$ dimensions) edits a specific attribute, we report scores for edits performed by the top 10 vectors with the highest singular values (top 10 for Greatest Hits and top 3 for Water Filling) for comparison in the table. (\uparrow) indicates higher values are better and scores

TABLE VII: Listening Test Results

| Water | | Greatest Hits | | |
|--------------------------|--------------------------|--------------------|---------------------------|------------------------|
| Fill Level(\uparrow) | Brightness(\uparrow) | Rate(\uparrow) | Impact Type(\uparrow) | |
| SeFa | 0.47 \pm 0.03 | 0.75 \pm 0.03* | 0.58 \pm 0.04 | 0.51 \pm 0.04 |
| Ours | 0.55 \pm 0.03 | 0.75 \pm 0.04* | 0.68 \pm 0.04 | 0.67 \pm 0.05 |

highlighted with "*" indicates no significant differences ($p > 0.05$). Each row indicates a semantic attribute manipulation using a specific guidance vector and each column evaluates how the scores changed for that attribute. The darkened cells in the table indicate dimensions with the highest score for a semantic attribute (in that column).

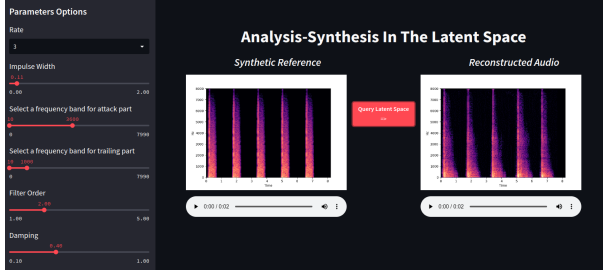
For both datasets, our method reports a significant change in the main attribute being manipulated. Further, we analyse if each dimension or direction vector from both methods manipulates only a single attribute. For this, we perform a two-way t-test for the scores between any two SeFa dimensions. We particularly notice that for SeFa, the semantic attribute of *Impact Type* is affected by at least two dimension vectors, namely Dimension 2 and Dimension 7 in Table V. This implies that methods such as SeFa may not always guarantee one-to-one correspondence between statistically found vectors for guidance and the semantic attributes of interest. Furthermore, the first dimension associated with the largest singular value extracted using SeFa does not correlate with any of the main perceptually varying attributes in both datasets. This implies that such automated methods do not always guarantee to find vectors that control perceptually relevant attributes in the latent space of a generative model for audio.

3) *Listening tests*: We recruited 20 participants on Amazon's Mechanical Turk to evaluate the sounds modified by using both methods. For the Greatest Hits dataset, we randomly sampled 20 sounds from the StyleGAN2's latent space and modified them using vectors derived using our method for *Brightness*, *Impact Type* and *Rate*. For SeFa, we used the vectors with the highest rescoring accuracy from Table V to manipulate the samples. The participants were presented with the unmodified original reference sound as well as the manipulated samples. They were asked to evaluate if the two samples differed on the 3 attributes. For the Water dataset, we randomly sampled the latent space 10 times and modified the samples using vectors for *Fill-Level*. As the *Fill-Level* for Water varies continuously, we wanted to evaluate if manipulating the sound samples sequentially and linearly using both methods preserves the interim *Fill-Levels* (such as when the bucket is empty, quarter or half full etc.). To do this, we use the rank-ordering interfaces outlined in [77] to measure the perceptual linearity of linearly manipulating the sample

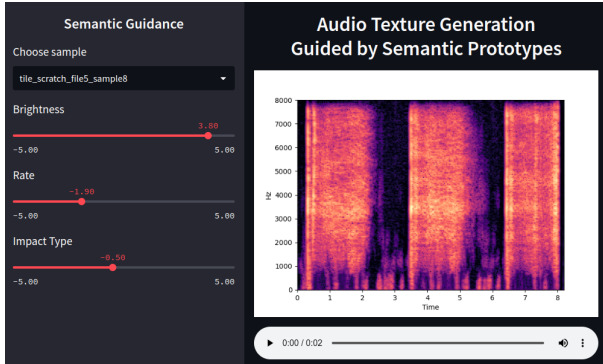
using the guidance vector for *Fill-Level*. The interfaces for the listening tests can be viewed on our supplementary webpage.

Table VII shows the accuracy scores from our listening tests for both datasets and their respective attributes. (\uparrow) indicates that higher values are better and scores highlighted with “*” indicates no significant differences ($p > 0.05$). For Water, participants were able to perceptually rank-order the water filling sounds in increasing order of *Fill-Level* significantly better when using our method. For the Greatest Hits dataset, participants found our method to perform significantly better while manipulating the sounds for *Rate* and *Impact Type*. However, for the attribute of *Brightness* participants found both methods to perform equally well. By qualitatively listening and comparing the brightness samples generated by the two algorithms, we find that samples generated using our method cover a wider range of brightness as compared to SeFa (visit the supplementary webpage for examples).

4) *Interactive editing with semantic guidance*: To qualitatively demonstrate the simplicity and effectiveness of our method, we developed two interfaces - (1) to query in real-time the latent space of a StyleGAN2 using synthetic sounds shown in Figure 4a, and (2) to interactively and in real-time semantically control generation of novel textures shown in Figure 4b. A video demonstration of our interfaces can be viewed on our supplementary webpage.



(a)



(b)

Fig. 4: Screenshots of an interface to(a) query a GAN’s latent space (b) guided generation using using our method.

V. APPLICATION: SELECTIVE SEMANTIC ATTRIBUTE TRANSFER

The prototypes and guidance vectors derived using our method also support applications such as selective semantic

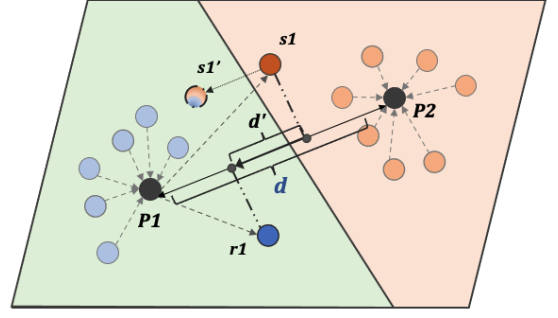


Fig. 5: Semantic attribute transfer from a reference to a target

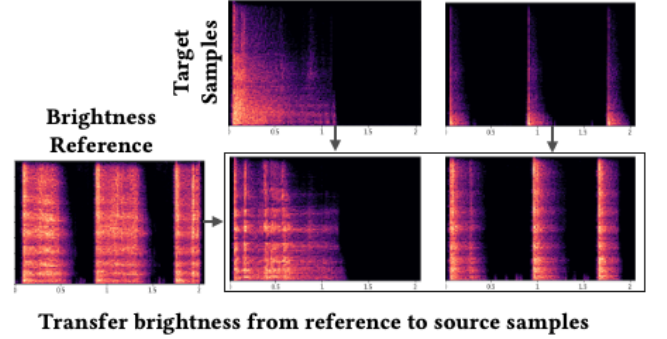


Fig. 6: Application of our method to selectively transfer brightness from ‘Brightness Reference’ to a ‘Target Sample’.

attribute transfer. This task is inspired from image editing applications such as photoshop, where a user can select an object and transfer its color to another object. We envision a selective attribute transfer tool where the prototype and guidance vectors guide the process of selecting an attribute from a reference sample and transferring it to another sample.

Algorithm 3: Transfer Semantic Attribute

Input:

- w encoded target sample to be modified;
- w_{ref} encoded reference sample;
- $w_{prototype}$ encoded concept prototype;
- d direction vector for concept;

Output:

$G_s(w)$ audio sample

Function $TransferAttribute(w, w_{ref}, w_{prototype}, d)$:

```

 $w_{projection} \leftarrow (w_{prototype} - w) \cdot d;$ 
 $ref_{projection} \leftarrow (w_{prototype} - w_{ref}) \cdot d;$ 
 $w \leftarrow w + (w_{projection} - ref_{projection}) * d;$ 
return  $G_s(w)$  ;  $\triangleright G_s(\cdot)$  denotes synthesis network

```

Figure 5 shows a diagram outlining the approach. Say we have a reference sample $r1$ and a target sample $s1$, and we want to selectively transfer the attribute of *Brightness* from the reference sample $r1$ to $s1$. To do this, we first project both $r1$ and $s1$ onto the attribute guidance vector between $P1$ and $P2$. We then edit $s1$ in the direction of the difference d' to create $s1'$. This method not only transfers the *Brightness* attribute from $r1$ to $s1'$, but also preserves the other unmodified

semantic attributes of *sI* as well as its original structure (position or location of the impact events along the time axis). The method to transfer semantic attribute is outlined in Algorithm 3. Results are shown in Figure 6 and our webpage.

VI. CONCLUSION

In this paper, we propose an audio example-based method to perceptually and deterministically guide generation of audio textures. By using a synthesizer to create a few examples, we are able to develop attribute guidance vectors in the latent space of a StyleGAN2 to controllably generate both discrete impact sounds as well as continuously varying water filling audio textures. We show the effectiveness of our method in providing linearly varying controls for texture generation using both objective metrics as well as perceptual listening tests. Furthermore, we demonstrate an application of our method to other signal processing tasks, namely semantic attribute transfer.

Although our method has been more effective than algorithms such as SeFa at modifying the user-defined semantic attributes on a texture, some manual curation of synthetic samples is needed to find the relevant guidance vectors. On the other hand, algorithms such as SeFa are automatic and can be applied to any pre-trained GAN without any manual intervention. Thus in our future work we will explore the potential of combining SeFa’s ability to automatically discover vectors for attribute manipulation with our method for improving the accuracy of editing the semantic attributes.

REFERENCES

- [1] J. H. McDermott and E. P. Simoncelli, “Sound texture perception via statistics of the auditory periphery: evidence from sound synthesis,” *Neuron*, vol. 71, no. 5, pp. 926–940, 2011.
- [2] N. Saint-Arnaud and K. Popat, *Analysis and Synthesis of Sound Textures*. USA: L. Erlbaum Associates Inc., 1998, p. 293–308.
- [3] D. B. Anderson and M. A. Casey, “The sound dimension,” *IEEE spectrum*, vol. 34, no. 3, pp. 46–50, 1997.
- [4] D. Moffat, R. Selfridge, and J. D. Reiss, “Sound effect synthesis,” in *Foundations in Sound Design for Interactive Media*. Routledge, 2019, pp. 274–299.
- [5] A. Wiener, “The weird, analog delights of foley sound effects,” 2022. [Online]. Available: <https://www.newyorker.com/magazine/2022/07/04/the-weird-analog-delights-of-foley-sound-effects>
- [6] I. J. Goodfellow, “NIPS 2016 tutorial: Generative adversarial networks,” *arXiv preprint arXiv:1701.00160*, vol. abs/1701.00160, 2017.
- [7] T. Karras, S. Laine, M. Aittala, J. Hellsten, J. Lehtinen, and T. Aila, “Analyzing and improving the image quality of stylegan,” in *Proceedings of the IEEE/CVF conference on computer vision and pattern recognition*, 2020, pp. 8110–8119.
- [8] T. Karras, S. Laine, and T. Aila, “A style-based generator architecture for generative adversarial networks,” in *Proceedings of the IEEE/CVF conference on computer vision and pattern recognition*, 2019, pp. 4401–4410.
- [9] E. Härkönen, A. Hertzmann, J. Lehtinen, and S. Paris, “Ganspace: Discovering interpretable gan controls,” *Advances in Neural Information Processing Systems*, vol. 33, pp. 9841–9850, 2020.
- [10] Y. Shen and B. Zhou, “Closed-form factorization of latent semantics in gans,” in *Proceedings of the IEEE/CVF Conference on Computer Vision and Pattern Recognition (CVPR)*, June 2021, pp. 1532–1540.
- [11] K. N. Watcharasupat, “Controllable music: supervised learning of disentangled representations for music generation,” 2021.
- [12] F. Kreuk, G. Synnaeve, A. Polyak, U. Singer, A. Défossez, J. Copet, D. Parikh, Y. Taigman, and Y. Adi, “Audiogen: Textually guided audio generation,” in *The Eleventh International Conference on Learning Representations*, 2023.
- [13] Z. Borsos, R. Marinier, D. Vincent, E. Kharitonov, O. Pietquin, M. Sharifi, D. Roblek, O. Teboul, D. Grangier, M. Tagliasacchi, and N. Zeghidour, “Audioldm: A language modeling approach to audio generation,” *IEEE/ACM Transactions on Audio, Speech, and Language Processing*, vol. 31, pp. 2523–2533, 2023.
- [14] A. Agostinelli, T. I. Denk, Z. Borsos, J. Engel, M. Verzetti, A. Caillon, Q. Huang, A. Jansen, A. Roberts, M. Tagliasacchi, M. Sharifi, N. Zeghidour, and C. Frank, “Musiclm: Generating music from text,” 2023.
- [15] H. Liu, Z. Chen, Y. Yuan, X. Mei, X. Liu, D. Mandic, W. Wang, and M. D. Plumbley, “Audioldm: Text-to-audio generation with latent diffusion models,” *arXiv preprint arXiv:2301.12503*, 2023.
- [16] B. Elizalde, S. Deshmukh, M. A. Ismail, and H. Wang, “Clap: Learning audio concepts from natural language supervision,” *arXiv preprint arXiv:2206.04769*, 2022.
- [17] A. Guzhov, F. Raue, J. Hees, and A. Dengel, “Audioclip: Extending clip to image, text and audio,” in *ICASSP 2022-2022 IEEE International Conference on Acoustics, Speech and Signal Processing (ICASSP)*. IEEE, 2022, pp. 976–980.
- [18] P. Grosche, M. Müller, and J. Serra, “Audio content-based music retrieval,” in *Dagstuhl Follow-Ups*, vol. 3. Schloss Dagstuhl-Leibniz-Zentrum für Informatik, 2012.
- [19] J. T. Foote, “Content-based retrieval of music and audio,” in *Multimedia storage and archiving systems II*, vol. 3229. SPIE, 1997, pp. 138–147.
- [20] A. Wang, “The shazam music recognition service,” *Communications of the ACM*, vol. 49, no. 8, pp. 44–48, 2006.
- [21] W. P. Birmingham, “MUSART: music retrieval via aural queries,” in *ISMIR 2001, 2nd International Symposium on Music Information Retrieval*, Indiana University, Bloomington, Indiana, USA, October 15–17, 2001, *Proceedings*, 2001.
- [22] A. Ghias, J. Logan, D. Chamberlin, and B. C. Smith, “Query by humming: Musical information retrieval in an audio database,” in *Proceedings of the third ACM international conference on Multimedia*, 1995, p. 231–236.
- [23] M. Cartwright and B. Pardo, “Synthassist: An audio synthesizer programmed with vocal imitation,” in *Proceedings of the 22nd ACM International Conference on Multimedia*, ser. MM ’14. New York, NY, USA: Association for Computing Machinery, 2014, p. 741–742.
- [24] B. Kim and B. Pardo, “Improving content-based audio retrieval by vocal imitation feedback,” in *ICASSP 2019-2019 IEEE International Conference on Acoustics, Speech and Signal Processing (ICASSP)*. IEEE, 2019, pp. 4100–4104.
- [25] Y. Zhang, B. Pardo, and Z. Duan, “Siamese style convolutional neural networks for sound search by vocal imitation,” *IEEE/ACM Transactions on Audio, Speech, and Language Processing*, vol. 27, no. 2, pp. 429–441, 2018.
- [26] J. Engel, K. K. Agrawal, S. Chen, I. Gulrajani, C. Donahue, and A. Roberts, “GANSynth: Adversarial neural audio synthesis,” in *International Conference on Learning Representations*, 2019.
- [27] J. Engel, L. H. Hantrakul, C. Gu, and A. Roberts, “Ddsp: Differentiable digital signal processing,” in *International Conference on Learning Representations*, 2020.
- [28] J. Engel, C. Resnick, A. Roberts, S. Dieleman, M. Norouzi, D. Eck, and K. Simonyan, “Neural audio synthesis of musical notes with wavenet autoencoders,” in *International Conference on Machine Learning*. PMLR, 2017, pp. 1068–1077.
- [29] A. Marafioti, N. Perraudin, N. Holighaus, and P. Majdak, “Adversarial generation of time-frequency features with application in audio synthesis,” in *International conference on machine learning*. PMLR, 2019, pp. 4352–4362.
- [30] L. Wyse, “Real-valued parametric conditioning of an RNN for interactive sound synthesis,” *arXiv preprint arXiv:1805.10808*, vol. abs/1805.10808, 2018. [Online]. Available: <http://arxiv.org/abs/1805.10808>
- [31] A. v. d. Oord, S. Dieleman, H. Zen, K. Simonyan, O. Vinyals, A. Graves, N. Kalchbrenner, A. Senior, and K. Kavukcuoglu, “WaveNet: A Generative Model for Raw Audio,” in *Proc. 9th ISCA Workshop on Speech Synthesis Workshop (SSW 9)*, 2016, p. 125.
- [32] P. Dhariwal, H. Jun, C. Payne, J. W. Kim, A. Radford, and I. Sutskever, “Jukebox: A generative model for music,” *arXiv preprint arXiv:2005.00341*, 2020.
- [33] Y.-S. Huang and Y.-H. Yang, “Pop music transformer: Beat-based modeling and generation of expressive pop piano compositions,” in *Proceedings of the 28th ACM International Conference on Multimedia*, 2020, pp. 1180–1188.
- [34] A. Roberts, J. Engel, C. Raffel, C. Hawthorne, and D. Eck, “A hierarchical latent vector model for learning long-term structure in music,” in *Proceedings of the 35th International Conference on Machine Learning*, ser. *Proceedings of Machine Learning Research*, J. Dy and A. Krause, Eds., vol. 80. PMLR, 10–15 Jul 2018, pp. 4364–4373.

- [35] C. Donahue, J. McAuley, and M. Puckette, "Adversarial audio synthesis," in *International Conference on Learning Representations*, 2019.
- [36] C. Y. Lee, A. Toffy, G. J. Jung, and W.-J. Han, "Conditional wavenet," *arXiv preprint arXiv:1809.10636*, 2018.
- [37] J. F. Gemmeke, D. P. Ellis, D. Freedman, A. Jansen, W. Lawrence, R. C. Moore, M. Plakal, and M. Ritter, "Audio set: An ontology and human-labeled dataset for audio events," in *2017 IEEE international conference on acoustics, speech and signal processing (ICASSP)*. IEEE, 2017, pp. 776–780.
- [38] J. Nistal, S. Lattner, and G. Richard, "Drumgan: Synthesis of drum sounds with timbral feature conditioning using generative adversarial networks," in *International Society for Music Information Retrieval Conference*, 2020.
- [39] T. Karras, T. Aila, S. Laine, and J. Lehtinen, "Progressive growing of GANs for improved quality, stability, and variation," in *International Conference on Learning Representations*, 2018.
- [40] M. T. Group, "Audio commons audio extractor," 2018. [Online]. Available: <https://www.audiocommons.org/2018/07/15/audio-commons-audio-extractor.html>
- [41] —, "Essentia: Open-source c++ library for audio analysis and audio-based music information retrieval," 2022. [Online]. Available: <https://essentia.upf.edu/>
- [42] J. Nistal, S. Lattner, and G. Richard, "Darkgan: Exploiting knowledge distillation for comprehensible audio synthesis with gans," in *International Society for Music Information Retrieval Conference*, 2021.
- [43] Q. Kong, Y. Cao, T. Iqbal, Y. Wang, W. Wang, and M. D. Plumbley, "Panns: Large-scale pretrained audio neural networks for audio pattern recognition," *IEEE/ACM Transactions on Audio, Speech, and Language Processing*, vol. 28, pp. 2880–2894, 2020.
- [44] P. Esling, A. Chemla-Romeu-Santos, and A. Bitton, "Bridging audio analysis, perception and synthesis with perceptually-regularized variational timbre spaces," in *Proceedings of the 19th International Society for Music Information Retrieval Conference, ISMIR 2018, Paris, France, September 23-27, 2018*, 2018, pp. 175–181.
- [45] P. Esling, A. Chemla-Romeu-Santos, and A. Bitton, "Generative timbre spaces: regularizing variational auto-encoders with perceptual metrics," *arXiv preprint arXiv:1805.08501*, 2018.
- [46] G. Gupta, P. Kamath, Y. Wei, Z. Li, S. Nanayakkara, and L. Wyse, "Towards controllable audio texture morphing," in *ICASSP 2023-2023 IEEE International Conference on Acoustics, Speech and Signal Processing (ICASSP)*. IEEE, 2023, pp. 1–5.
- [47] L. Wyse, P. Kamath, and C. Gupta, "Sound model factory: An integrated system architecture for generative audio modelling," in *Artificial Intelligence in Music, Sound, Art and Design: 11th International Conference, EvoMUSART 2022, Held as Part of EvoStar 2022, Madrid, Spain, April 20–22, 2022, Proceedings*. Springer, 2022, pp. 308–322.
- [48] Y. Shen, C. Yang, X. Tang, and B. Zhou, "Interfacegan: Interpreting the disentangled face representation learned by gans," *IEEE transactions on pattern analysis and machine intelligence*, vol. 44, no. 4, pp. 2004–2018, 2020.
- [49] A. Voynov and A. Babenko, "Unsupervised discovery of interpretable directions in the GAN latent space," in *Proceedings of the 37th International Conference on Machine Learning*, ser. Proceedings of Machine Learning Research, H. D. III and A. Singh, Eds., vol. 119. PMLR, 13–18 Jul 2020, pp. 9786–9796.
- [50] Z. Wu, D. Lischinski, and E. Shechtman, "Stylespace analysis: Disentangled controls for stylegan image generation," in *Proceedings of the IEEE/CVF Conference on Computer Vision and Pattern Recognition (CVPR)*. Virtual: CVPR, June 2021, pp. 12 863–12 872.
- [51] Y. Shen, J. Gu, X. Tang, and B. Zhou, "Interpreting the latent space of gans for semantic face editing," in *Proceedings of the IEEE/CVF conference on computer vision and pattern recognition*. CVPR, 2020, pp. 9243–9252.
- [52] K. Tahiroglu, M. Kastemaa, and O. Koli, "Ganspacesynth: A hybrid generative adversarial network architecture for organising the latent space using a dimensionality reduction for real-time audio synthesis," in *Proceedings of the 2nd Joint Conference on AI Music Creativity*, 2021.
- [53] K. N. Haque, R. Rana, J. Liu, J. H. L. Hansen, N. Cummins, C. Busso, and B. W. Schuller, "Guided generative adversarial neural network for representation learning and audio generation using fewer labelled audio data," *IEEE/ACM Transactions on Audio, Speech, and Language Processing*, vol. 29, pp. 2575–2590, 2021.
- [54] K. N. Haque, R. Rana, and B. W. Schuller, "High-fidelity audio generation and representation learning with guided adversarial autoencoder," *IEEE Access*, vol. 8, pp. 223 509–223 528, 2020.
- [55] R. Parihar, A. Dhiman, T. Karmali, and V. R., "Everything is there in latent space: Attribute editing and attribute style manipulation by stylegan latent space exploration," in *Proceedings of the 30th ACM International Conference on Multimedia*, ser. MM '22. New York, NY, USA: Association for Computing Machinery, 2022, p. 1828–1836.
- [56] W. Xia, Y. Zhang, Y. Yang, J.-H. Xue, B. Zhou, and M.-H. Yang, "Gan inversion: A survey," *IEEE Transactions on Pattern Analysis and Machine Intelligence*, 2022.
- [57] L. Chai, J. Wulff, and P. Isola, "Using latent space regression to analyze and leverage compositionality in gans," in *International Conference on Learning Representations*. Virtual Only: ICLR, 2021.
- [58] J. Snell, K. Swersky, and R. Zemel, "Prototypical networks for few-shot learning," in *Advances in Neural Information Processing Systems*, I. Guyon, U. V. Luxburg, S. Bengio, H. Wallach, R. Fergus, S. Vishwanathan, and R. Garnett, Eds., vol. 30. Curran Associates, Inc., 2017.
- [59] J. O. Smith, *Spectral Audio Signal Processing*. <http://ccrma.stanford.edu/~jos/sasp/>, April 2023, online book, 2011 edition.
- [60] X. Serra and J. Smith, "Spectral modeling synthesis: A sound analysis/synthesis system based on a deterministic plus stochastic decomposition," *Computer Music Journal*, vol. 14, no. 4, pp. 12–24, 1990.
- [61] X. Serra, *A system for sound analysis/transformation/synthesis based on a deterministic plus stochastic decomposition*. Stanford University, 1990.
- [62] X. Serra *et al.*, "Musical sound modeling with sinusoids plus noise," *Musical signal processing*, pp. 91–122, 1997.
- [63] J. O. Smith, *Physical Audio Signal Processing*. <http://ccrma.stanford.edu/~jos/pasp/>, April 2023, online book, 2010 edition.
- [64] W. W. Gaver, "What in the world do we hear?: An ecological approach to auditory event perception," *Ecological psychology*, vol. 5, no. 1, pp. 1–29, 1993.
- [65] —, "How do we hear in the world? explorations in ecological acoustics," *Ecological psychology*, vol. 5, no. 4, pp. 285–313, 1993.
- [66] P.-Y. Huang, H. Xu, J. Li, A. Baevski, M. Auli, W. Galuba, F. Metze, and C. Feichtenhofer, "Masked autoencoders that listen," *Advances in Neural Information Processing Systems*, vol. 35, pp. 28 708–28 720, 2022.
- [67] D. Niizumi, D. Takeuchi, Y. Ohishi, N. Harada, and K. Kashino, "Masked spectrogram modeling using masked autoencoders for learning general-purpose audio representation," in *HEAR: Holistic Evaluation of Audio Representations*. PMLR, 2022, pp. 1–24.
- [68] R. Zhang, P. Isola, A. A. Efros, E. Shechtman, and O. Wang, "The unreasonable effectiveness of deep features as a perceptual metric," in *Proceedings of the IEEE conference on computer vision and pattern recognition*, 2018, pp. 586–595.
- [69] J. Antognini, M. Hoffman, and R. J. Weiss, "Synthesizing diverse, high-quality audio textures," *arXiv preprint arXiv:1806.08002*, 2018.
- [70] A. Owens, P. Isola, J. McDermott, A. Torralba, E. H. Adelson, and W. T. Freeman, "Visually indicated sounds," in *2016 IEEE Conference on Computer Vision and Pattern Recognition (CVPR)*. Los Alamitos, CA, USA: IEEE Computer Society, jun 2016, pp. 2405–2413.
- [71] C. Gupta, Y. Wei, Z. Gong, P. Kamath, Z. Li, and L. Wyse, "Parameter sensitivity of deep-feature based evaluation metrics for audio textures," in *Proceedings of the 23rd International Society for Music Information Retrieval Conference, ISMIR 2022, Bengaluru, December 4-8, 2022*, 2022, pp. 462–468.
- [72] Z. Prusa, P. Balazs, and P. L. Sondergaard, "A noniterative method for reconstruction of phase from stft magnitude," *IEEE/ACM Transactions on Audio, Speech, and Language Processing*, vol. 25, no. 5, pp. 1154–1164, 2017.
- [73] C. Gupta, P. Kamath, and L. Wyse, "Signal representations for synthesizing audio textures with generative adversarial networks," *arXiv preprint arXiv:2103.07390*, 2021.
- [74] K. He, X. Zhang, S. Ren, and J. Sun, "Deep residual learning for image recognition," in *Proceedings of the IEEE conference on computer vision and pattern recognition*, 2016, pp. 770–778.
- [75] K. Kilgour, M. Zuluaga, D. Roblek, and M. Sharifi, "Fréchet audio distance: A reference-free metric for evaluating music enhancement algorithms," in *INTERSPEECH*, 2019, pp. 2350–2354.
- [76] K. Palanisamy, D. Singhania, and A. Yao, "Rethinking CNN models for audio classification," *CoRR*, vol. abs/2007.11154, 2020.
- [77] P. Kamath, Z. Li, C. Gupta, K. Jaidka, S. Nanayakkara, and L. Wyse, "Evaluating descriptive quality of ai-generated audio using image-schemas," in *Proceedings of the 28th International Conference on Intelligent User Interfaces*, ser. IUI '23. New York, NY, USA: Association for Computing Machinery, 2023, p. 621–632.